NO Adsorption on MoS_x Clusters: A Density Functional Theory Study

Xiao-Dong Wen,[†] Yong-Wang Li,[†] Jianguo Wang,[†] and Haijun Jiao*[,†,‡]

State Key laboratory of Coal Conversion, Institute of Coal Chemistry, Chinese Academy of Sciences, Taiyuan, Shanxi 030001, P. R. China; Leibniz-Institut für Katalyse e.V. an der Universität Rostock, Albert-Einstein-Strasse 29a, 18059 Rostock, Germany

Received: February 4, 2006; In Final Form: July 30, 2006

The density functional theory (DFT) method has been used to investigate NO probe molecule adsorption on the stoichiometric ($Mo_{16}S_{32}$) and nonstoichiometric ($Mo_{16}S_{34}$ and $Mo_{16}S_{29}$) clusters. The calculated adsorption energies indicate that the stoichiometric cluster has stronger NO affinity than the nonstoichiometric surfaces. It is also found that mononitrosyl adsorption is favored at low NO coverage, while dinitrosyl (germinal) and $(NO)_2$ dimer adsorption at high NO coverage are possible. Strong repulsive interaction has been found for the adsorbed dinitrosyl and $(NO)_2$ dimer species. In addition, the computed NO stretching frequencies for the mononitrosyl and dinitrosyl species agree well with the experimental data, while those of the dimer species are much lower than the suggested experimental data.

1. Introduction

Molybdenum sulfides (MoS_x) are widely used catalysts in oil refining for hydrogenation, hydrodesulfurization, and hydrodenitrogenation reactions for producing clean fuels. Characterization techniques and activity investigations have provided insights into the nature of the active phases on MoS_x catalysts. However, the increasing demands for cleaner fuels (lower sulfur content) need hydrotreating catalysts with higher activity and selectivity, and consequently, a rationalized understanding of the activity and surface structure of MoS_x catalysts is essential.

Many spectroscopic techniques have been used to characterize MoS_x catalysts, e.g., scanning electron microscopy,[1] transmission electron spectroscopy,[2] X-ray photoelectron spectroscopy,[3] extended X-ray photoelectron spectroscopy[4] and scanning tunneling microscopy.[5] However, most of these methods do not provide direct information about the exposed or coordinatively unsaturated surface atoms, while characterization of active species by using adsorbed probe molecules is informative, especially when the fraction of the active species is very small. Infrared (IR) spectroscopy is widely used to detect the adsorbed probe molecules on the surface of catalysts. Chemisorption of CO molecule provides important insights into the surface structure of the active sites of MoS_x. IR study of adsorbed NO reveals the properties of the exposed surface structures, and NO chemisorption is very informative and useful to distinguish the coordinatively unsaturated Mo sites on MoS_x catalysts and the promotion Co (Ni) sites in the case of MoS_x catalysts.

The surface structures of the active sites of MoS_x catalysts have been studied by using a NO probe molecule.[6−12] Okamoto et al.[8] found two frequencies (1780 and 1680 cm^{-1}) for the adsorbed NO on the sulfided MoO_3/Al_2O_3 catalysts. These frequencies are characteristic for dinitrosyl species and lower than those (1820 and 1710 cm^{-1}) on the MoO_3/Al_2O_3 catalysts reduced by H_2. Their results indicate that the the NO/Mo ratio depends linearly on the vacancy concentration on Mo and two NO molecules can adsorb on a single Mo site to form dinitrosyl complex. IR study of NO adsorption on the sulfided Mo/Al_2O_3 catalysts evidenced the formation of dinitrosyl species.[6,7,9] Valyon et al.[9,10] reported that dinitrosyl species on the sulfided Mo/Al_2O_3 catalysts at 1795 and 1704 cm^{-1} for the symmetric and asymmetric NO stretching vibrations, respectively. X-ray photoelectron spectroscopy study on the adsorbed NO on MoS_x by Shuxian et al.[11] suggested the formation of two distinct NO species. Maugé et al.[12] studied the surface properties of unsupported MoS_x catalysts with the help of NO as a probe molecule and found a couple of NO bands at 1855 and 1756 cm^{-1}, which are attributed to the dinitrosyl species weakly bound to the surface, and the broader band at 1775 and 1675 cm^{-1} corresponds to the adsorbed $(NO)_2$ dimer species. As one can see, the frequencies for dinitrosyl and dimer species are discussed controversially.

In addition, the active sites of the sulfided $CoMo/Al_2O_3$ and $NiMo/Al_2O_3$ catalysts have been studied with NO probes.[13−17] On the basis of NO adsorption, Topsøe et al.[13] found that the promoted Co atoms locate in the Co−Mo−S phase. Okamoto et al.[16] proposed that the structure of the Co−Mo−S phase has Co−S−Co clusters located on the edge of MoS_x particles. The FT-IR spectra of NO adsorption on $Co/MoS_2/Al_2O_3$ showed a set of intense double bands at 1845 and 1785 cm^{-1}, which are characteristic for NO molecules adsorbed on Co sites in a dinitrosyl form.[16,17]

NO adsorption on other surfaces has been widely studied. Schönnenbeck et al.[18] found that the NO stretching frequency on NiO and CoO was shifted toward lower frequencies compared to the gas-phase value. Nart et al.[19] and Queeney et al.[20] studied NO adsorption and reactivity on the oxidized Mo(110) and found the formation of mononitrosyl and dinitrosyl species at low and saturated coverages, respectively. Zecchina et al.[21] assigned the peak at 1810 cm^{-1} for mononitrosyl adsorption on supported catalysts containing Cr and peaks at 1747 and 1865 cm^{-1} for $[Cr(NO)_2]^{2+}$ as well as 1755 and 1880 cm^{-1} for $[Cr(NO)_2]^{3+}$ as dinitrosyl. Mononitrosyl and dinitrosyl adsorptions on Ag have been studied using the density functional theory (DFT) method by Liu et al.[22]

* Corresponding author. E-mail: haijun.jiao@ifok-rostock.de.
† State Key laboratory of Coal Conversion, Institute of Coal Chemistry.
‡ Leibniz-Institut für Katalyse e.V. an der Universität Rostock.

10.1021/jp060747x CCC: $33.50
Published on Web 09/26/2006

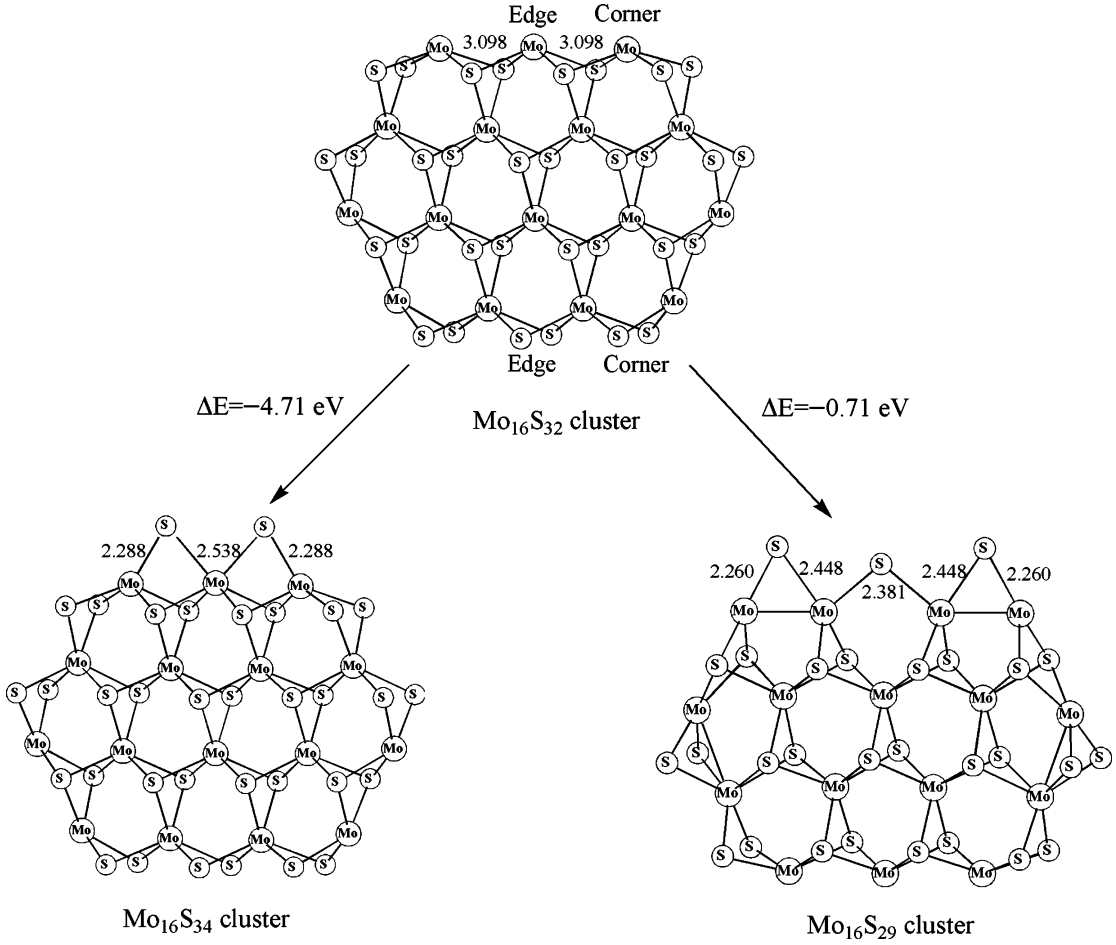

Figure 1. $Mo_{16}S_x$ model clusters: (a) $Mo_{16}S_{32}$ with 0% sulfur Mo edge and 100% sulfur S edge; (b) $Mo_{16}S_{34}$ with 33% sulfur Mo edge and 100% sulfur S edge; (c) $Mo_{16}S_{29}$ with 0% sulfur Mo edge and 50% sulfur S edge.

Despite the extensive and intensive studies, there are crucial problems unresolved for NO adsorption on HDS catalysts. For example, what are the detailed structures and energetic aspects of the adsorbed mononitrosyl and dinitrosyl? Is it possible for multiple NO adsorptions? How about the interaction of adsorbed dinitrosyl and dimer species? Here we present the DFT studies on NO adsorption on a set of stoichiometric and nonstoichiometric $Mo_{16}S_x$ clusters to understand the above-mentioned questions. Such clusters were used to study the CO adsorption on the corners and edges.[23,24]

2. Models and Methods

2.1. Models. In this work, we took three clusters to model the stoichiometric ($Mo_{16}S_{32}$) and nonstoichiometric ($Mo_{16}S_{34}$ and $Mo_{16}S_{29}$) MoS_x surfaces. The $Mo_{16}S_{32}$ cluster with 0% sulfur Mo edge and 100% sulfur S edge is shown in Figure 1. $Mo_{16}S_{34}$ has two bridge S atoms on the Mo edge (33% sulfur coverage on the Mo edge by adding two S atoms on the Mo edge) and $Mo_{16}S_{29}$ has three bridge S atoms on the S edge (50% sulfur coverage on the S edge by deleting three S atoms from the S edge). As found previously,[33] the formation of $Mo_{16}S_{34}$ with 33% sulfur coverage on the Mo edge is exothermic (−4.71 eV) from $Mo_{16}S_{32}$ with 0% sulfur coverage on the Mo edge. The smallest H_2S/H_2 ratio effect is found for 33% sulfur coverage on the Mo edge. $Mo_{16}S_{29}$ with 50% sulfur coverage on the S edge is the most stable structure; the formation energy of $Mo_{16}S_{29}$ is −0.71 eV from $Mo_{16}S_{32}$. In $Mo_{16}S_{32}$, the edge Mo−Mo distance is 3.098 Å. In $Mo_{16}S_{34}$, the Mo(c)−S (from corner Mo to S) and Mo(e)−S (from edge Mo to S) distances are 2.288 and 2.538 Å, respectively. In $Mo_{16}S_{29}$, the Mo(c)−S(c) (from corner Mo to corner S), Mo(e)−S(c) (from edge Mo to corner S) and Mo(e)−S(e) (from edge Mo to edge S) distances are 2.260, 2.448, and 2.381 Å, respectively.

There are intensive investigations into the surface structure and stability of MoS_x catalysts. For MoS_x catalysts, Lauritsen et al.[25] have provided insights into the atomic-scale structure and morphology of MoS_x nanoclusters by scanning tunneling microscopy (STM) and found that the morphology of MoS_x nanoclusters as catalysts may in fact be very complex. By using the DFT method, Byskov et al.,[26] Raybaud et al.,[27,28] Cristol et al.,[29,30] and Sun et al.[31,32] have reported the surface structures of MoS_x catalysts on the basis of the periodic model. Their results indicated that it is energetically unfavorable to obtain the Mo edge and S edge of MoS_x surfaces with sulfur coverage lower than 50%, and adding sulfur atoms to the bare Mo edge is an exothermic process up to 50% sulfur coverage. Recently, we have also studied the surface structure and stability of different MoS_x clusters instead of the periodic model by using the DFT method[33] and found that adding sulfur to the Mo edge is always exothermic and deleting corner sulfur from the S edge is exothermic for 67% and 50% sulfur coverage. However, our results do not agree fully with the results obtained by using the periodic slab model, which shows that the removal of sulfur from the S edge is always endothermic. This energetic difference originates from the difference of the cluster model and the period model. The cluster model has both edge and corner sulfur atoms, while the periodic model has only edge sulfurs. Removing corner sulfur is much easier than that of edge sulfur.

TABLE 1: Calculated NO Adsorption Energies on the $Mo_{16}S_{32}$ Cluster (E_{ads}, eV and ΔE_{ads}, eV), As Well As the NO Vibrational Frequency (cm^{-1})

model	E_{ads} (ΔE_{ads})	ν (NO)
	One NO Adsorption	
1	−3.19	1684
2	−3.49	1688
3	−3.56	1104
4	−3.79	1103
5	−0.81	1659
6	−0.71	1652
	Two NO Adsorption	
7	−6.39 (+0.29)	1676[a]/1726[b]
8	−6.28 (+0.10)	1682[a]/1697[b]
9	−6.80 (+0.18)	1095[a]/1706[b]
10	−6.06 (+1.52)	1087[a]/1100[b]
11	−3.89 (+2.49)	1735[a]/1776[b]
12	−3.64 (+3. 34)	1628[a]/1745[b]
13	−3.59 (+2.79)	1514[a]/1496[b]
14	−3.51 (+3.47)	1521[a]/1501[b]
15	−4.27 (+2.40)	1456[a]1430[b]
	Six NO Adsorption	
16	−10.34 (+1.08)	1753[a]/1815[b] (corner) 1708[a]/1768[b] (edge)
17	−10.21 (+0.48)	1595[a]/1577[b] (corner) 1570[a]/1539[b] (edge)
18	−11.29 (0.00)	1775[a]/1800[b] (corner) 1504[a]/1499[b] (edge)
19	−10.53 (+0.26)	1552[a]/1533[b] (corner) 1706[a]/1804[b] (edge)

[a] Asymmetric stretching frequencies. [b] Symmetric stretching frequencies.

In addition, formation of the bare Mo edge depends not only on the low H_2S/H_2 ratio, but also on the size of MoS_x clusters. Paul et al.[34] studied the vacancy formation mechanism on the Mo edge of the MoS_2 slab by using the periodic model and found that the activation energy of the rate-determining step of the vacancy formation remains less than 23 kcal/mol on the Mo edge. Recently, Zeng et al.[35] investigated the removal of bridging sulfur on the Mo edge of a $Mo_{20}S_{43}$ cluster with and without CO adsorption under the change of the CO/H_2S ratio, and they found that, on the basis of multiple or full CO adsorption and the availability of activated hydrogen on the nonstoichiometric hexagonal cluster, surface sulfur can be removed at very high CO/H_2S partial pressure with the formation of adsorbed CO on formally naked Mo edge. It is interesting to note that the reverse reaction, the removal of adsorbed CO by H_2S at very high H_2S/CO partial pressure, has been observed experimentally by Travert et al.[36] Therefore, the CO/H_2S exchange reaction could be adjusted by changing the CO/H_2S partial pressure, i.e., high CO/H_2S partial pressure leads to the removal of adsorbed H_2S, while low CO/H_2S partial pressure leads to the removal of adsorbed CO.

Our preliminary result shows that one H_2S removal from the Mo edge with 50% H_2S coverage needs about 20 kcal/mol to form the Mo edge with 33% H_2S coverage and the additional removal of H_2S to form a naked Mo edge needs about 28 kcal/mol. These energy costs are lower than the adsorption energies of one NO (up to 3.8 eV) or two NO probes (up to 6.8 eV) (see Table 1), and therefore, NO adsorption can help move H_2S and finally result in adsorbed NO on naked Mo edge despite the difficulty to get the naked Mo edge in an "isolated" state. Therefore, it is notable that the formation of the naked Mo edge is energetically not favored but the covered Mo edge with probe molecules (like CO and H_2S) can be formed indirectly. In addition, the naked Mo edge can provide the platform for comprehensive and systematic comparison and analysis of the catalytic properties of MoS_x catalysts.

2.2. Calculation Methods. All calculations were performed with the program package DMol[3] in the Materials Studio 2.2 of Accelrys Inc. The physical wave functions were expanded in terms of accurate numerical basis sets.[37] The doubled numerical basis set including polarization functions was used for other elements, while effective core potential was used for Mo. The generalized gradient corrected functional by Perdew and Wang (PW91)[38] was used, and the medium quality mesh size was used for numerical integration. The tolerances of energy, gradient, and displacement convergence were 2×10^{-5} au, 4×10^{-3} au/Å, and 5×10^{-3} Å, respectively. The real space cutoff of atomic orbitals was set at 5.5 Å, and a Fermi smearing of 0.0005 eV was used for orbital occupancy. Unrestricted spin polarization was used. The bare and adsorbed clusters as well as the probe molecules have been fully optimized and relaxed without any constraints.

For studying the interaction between NO and a surface, we used the adsorption energy in eq 1, in which E(cluster) and E(NO) are the energies of the bar cluster and free NO, respectively, while $E(NO)_n$/cluster is the energy of the adsorbed NO complex and n is the number of the adsorbed NO probes. On the basis of this equation, the more negative the adsorption energy, the stronger the adsorption.

$$E_{ads} = E((NO)_n/\text{cluster}) - [E(\text{cluster}) + nE(NO)] \quad (1)$$

To study the influence of the increased coverage, it is necessary to compare the difference (ΔE_{ads}) in adsorption energy between the higher coverage (E_{ads}, $n > 1$) and the sum of the single NO adsorption ($\sum E_{ads}$, $n = 1$). This is defined in eq 2.

$$\Delta E_{ads} = (E_{ads}, n > 1) - \sum (E_{ads}, n = 1) \quad (2)$$

The vibrational frequencies of the adsorbed NO were calculated by numerical differentiation of the force matrix. To reduce cost, we computed only the matrix corresponding to N and O. This simplified method has been used to compute the CO frequencies on MoS_x.[24] Comparison between the experimental (1880 cm^{-1}) and calculated stretching frequency (1890 cm^{-1}) for NO gives a ratio of 0.995, which is used to scale the calculated frequencies.

3. Results and Discussion

3.1. NO Adsorption on $Mo_{16}S_{32}$ Cluster. The $Mo_{16}S_{32}$ cluster with 0% sulfur Mo edge and 100% sulfur S edge is shown in Figure 1. NO adsorption on the two edges of $Mo_{16}S_{32}$ cluster is studied, and the optimized structures are shown in Figure 2. The adsorption energies (E_{ads}) are given in Table 1.

(a) One NO Adsorption. Four structures (**1**−**4**) with one adsorbed NO on the Mo edge (0% sulfur) are shown in Figure 2. As given in Table 1, all adsorptions are strongly exothermic, indicating the high NO affinity. Bridge adsorptions **3** and **4** (−3.56/−3.79 eV) are stronger than corner and edge adsorptions **1** and **2** (−3.19/−3.49 eV). The adsorption energy of **4** with the O atom bound to the corner Mo is higher than that of **3**, with the O atom bonded to the edge Mo. The adsorption energy of NO on the single edge Mo atom (**2**) is higher than that on the single corner Mo atom (**1**), and this is in line with CO adsorption.[23]

The structures (**5** and **6**) with NO adsorption on the S edge (100% sulfur) are shown in Figure 2. However, NO adsorption on the S edge (**5** and **6**) is much less favored, as indicated by the rather lower adsorption energies (−0.81 and −0.71 eV,

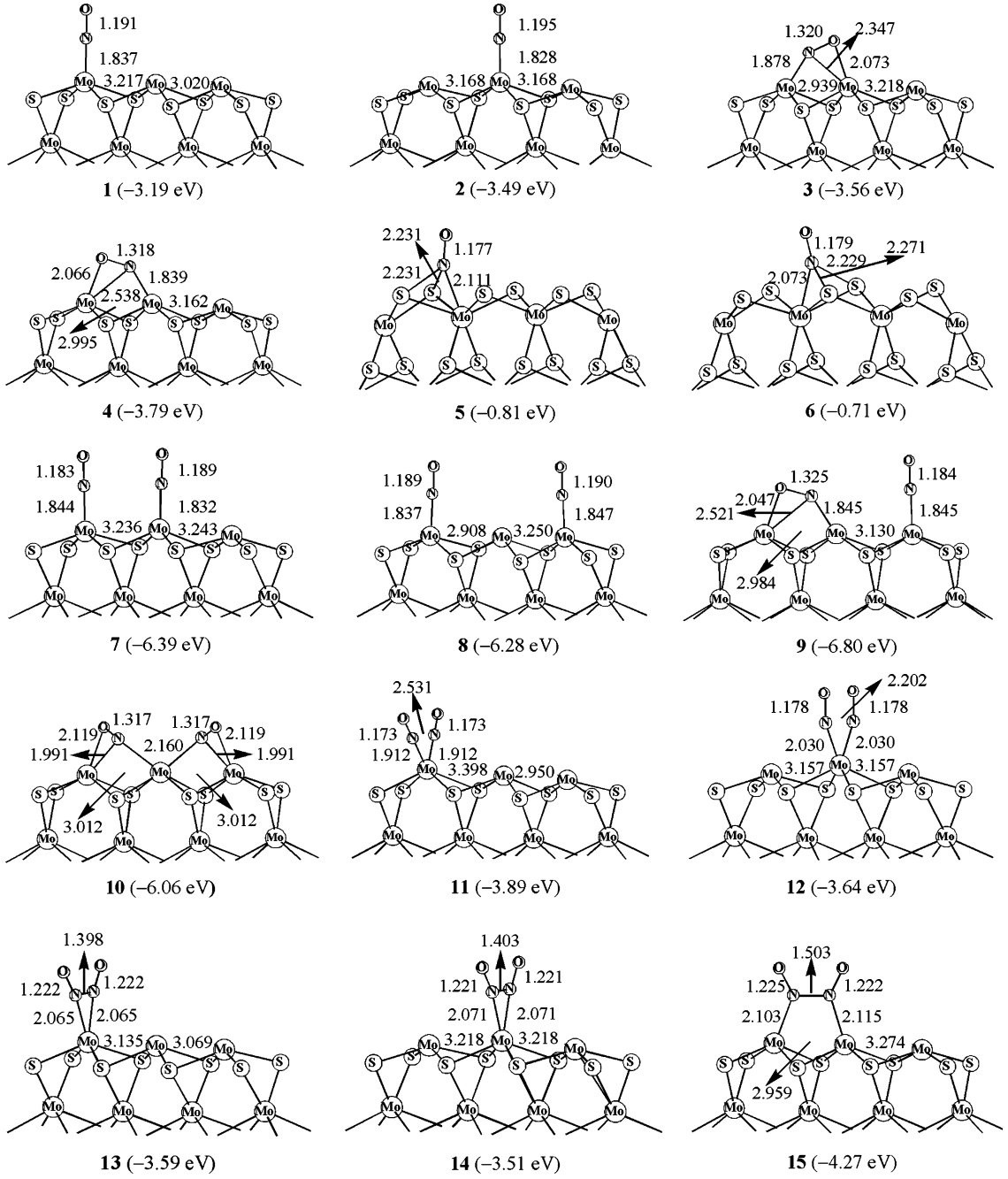

Figure 2. Optimized one NO (**1**−**6**) and two NO adsorption structures (**7**−**15**) on the $Mo_{16}S_{32}$ cluster.

respectively). The same situations also have been found for CO adsorption.[23] Therefore, we do not focus on the 100% sulfur S edge further.

In **1** and **2**, the Mo−N distances are 1.837 and 1.828 Å, and the N−O bond lengths are 1.191 and 1.195 Å, respectively (Figure 2). In **3** and **4**, the Mo(c)−N and Mo(e)−N distances are 1.878/2.347 Å, and 2.538/1.839 Å, respectively.

(b) Two NO Adsorption. Adsorption of two NO probes is also studied on the 0% sulfur Mo edge. There are nine adsorption structures (**7**−**15**) on the Mo edge, as shown in Figure 2. As given in Table 1, all adsorptions are exothermic. Structures **7** and **8** can be considered as the combination of **1** and **2**, and the adsorption energies of **7** and **8** are roughly close to the sum of **1** and **2** as well as two times **1** (−6.39 and −6.28 vs −6.68 and −6.38 eV, respectively). The same is also found for **9**, which can be considered as the combination of **1** and **4** in both geometry and energy (−6.80 vs −6.98 eV).

Structures **11** and **12** have dinitrosyl (germinal NO) adsorption on corner and edge Mo sites, respectively, but their adsorption energies (−3.82 and −3.10 eV, respectively) are much lower than the sum of two **1** and two **2** (−6.38 and −6.98 eV, respectively), indicating the strong repulsive interaction of the germinal adsorbed NO probes. This repulsive interaction is much stronger than that of germinal CO adsorption.[23] Apart from the terminal adsorption in **11** and **12**, it is interesting to note that there is also adsorption of the $(NO)_2$ dimer. Structures **13** and **14** have adsorbed $(NO)_2$ at the corner and edge Mo sites, while **15** has adsorbed $(NO)_2$ bridging corner and edge Mo sites. The N−N distances are 1.398 Å in **13** and 1.403 Å in **14**, but longer in **15** (1.503 Å). The adsorption energies (−3.59 and −3.51 eV, respectively) of **13** and **14** are lower than that (−4.27 eV) of **15**.

Among the nine structures of two adsorbed NO probes, the most stable adsorption form is **9** (−6.80 eV) with one bridge

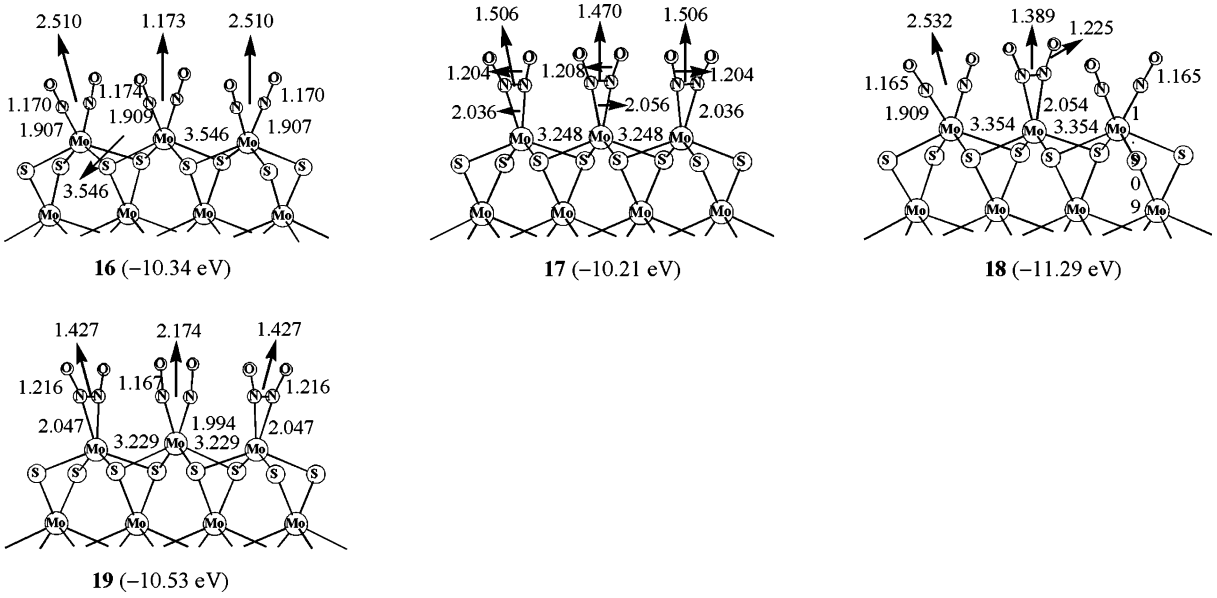

Figure 3. Optimized six NO adsorption structures on the $Mo_{16}S_{32}$ cluster.

NO and one top NO, followed by **7** (−6.39 eV) with two NO probes on one corner and edge Mo atom and by **8** (−6.28 eV) with two NO probes at two corner Mo sites. The other structures are much less stable. On the basis of these results, it is proposed that dinitrosyl and dimer species are less possible at low NO coverage.

(c) NO Adsorption at Higher Coverage. We have also computed full NO adsorption on the Mo site. As shown in Figure 3, both the corner and edge Mo sites can adsorb two NO in dinotrosyl and dimer forms. Structure **16** has six top-adsorbed NO (or three dinitrosyl) probes, while **17** has three adsorbed dimer species. Structure **18** has two dinitrosyl groups at the corner Mo sites and one dimer group at the edge Mo site. Structure **19** has two dimer groups at the corner sites and one dinitrosyl form at the edge site. As given in Table 1, the adsorption energies of **16**, **17**, **18**, and **19** are exothermic by 10.34, 10.21, 11.29 and 10.53 eV, respectively, indicating the thermodynamic possibility for full NO adsorption. It is interesting to note that the ΔE_{ads} values for **16** (+1.08 eV), **17** (+0.48 eV), and **19** (+0.26 eV) are positive as compared with those of the corresponding two corner and one edge adsorptions. However, the ΔE_{ads} value for **18** with dimer species adsorption is zero. On the basis of these results, both dinitrosyl and dimer adsorptions are favored at higher NO coverage, and therefore, NO concentration will control the adsorption structures.

The changes of the surface structure (Mo−Mo distance on $Mo_{16}S_{32}$ cluster) after adsorption also are shown in Figure 3. Compared to $Mo_{16}S_{32}$ (3.098 Å), the Mo−Mo distances after adsorption in **3**, **4**, **8**−**11**, and **15** are shorter, while in other structures, they are longer.

(d) NO Stretching Frequencies. The frequencies for all adsorbed NO probes are calculated. For one NO adsorption on the Mo edge, the stretching frequency (1104 and 1103 cm^{-1}, respectively) for bridge adsorption **3** and **4** is lower than that (1684 and 1688 cm^{-1}, respectively) for top adsorption **1** and **2**.

In two NO adsorption with two Mo atoms, the frequencies for the most stable adsorption **9** are 1095 (bridge) and 1706 (top) cm^{-1}, respectively. The frequencies of the top adsorbed NO in **7** and **8** are 1676 and 1682 cm^{-1}, respectively, for the asymmetric stretching, and 1726 and 1697 cm^{-1}, respectively, for the symmetric stretching. The frequencies of the most stable dinitrosyl **11** are 1735 and 1776 cm^{-1}, while those of the most stable dimer **15** are much lower (1456 and 1430 cm^{-1}).

Experimentally, Maugé et al.[12] ascribed the couple of NO IR bands at 1855 and 1756 cm^{-1} to the weakly bound dinitrosyl species on the surface of MoS_x and another pair of broader bands at 1775 and 1675 cm^{-1} to the $(NO)_2$ dimer species. In our calculation, the frequencies of **1** and **2** (1684 and 1688 cm^{-1}) are close to the characteristic 1675 cm^{-1}. However, the frequencies of the dinitrosyl species do not agree with the data (1855 and 1756 cm^{-1}) of Maugé et al.,[12] but agree with the data (1795 and 1704 cm^{-1}) of Valyon et al.[9,10] The frequencies of the dimer species range from 1539 to 1595 cm^{-1}, lower than these of dinitrosyl species. Therefore, the NO frequencies by Maugé et al.[12] may belong to the dinitrosyl species instead of the NO dimers.

3.2. NO Adsorption on $Mo_{16}S_{34}$ Cluster. Apart from the NO adsorption on $Mo_{16}S_{32}$, two nonstoichiometric clusters ($Mo_{16}S_{34}$ and $Mo_{16}S_{29}$) are used to model the NO adsorption on the changed surfaces. The optimized adsorption structures for one NO, two NO, and six NO molecules on the $Mo_{16}S_{34}$ cluster with 33% sulfur coverage of the S edge are shown in Figure 4, and the calculated adsorption energies are given in Table 2.

(a) One NO Adsorption. As shown in Figure 4, there are two adsorption structures in the $Mo_{16}S_{34}$ cluster for one NO adsorption, e.g., at the corner Mo atom (**20**) and at the edge Mo atom (**21**). However, it is not possible to get the bridge adsorption on one corner Mo atom and one edge Mo atom, and optimization led to **20**. As given in Table 2, **20** (−1.96 eV) with NO adsorption on the corner is more favorable than **21** (−1.79 eV) with NO adsorption on the edge, in which the two sulfur bridges are converted into terminal sulfurs. The change of **21** indicate that NO creates its own adsorption site. This agrees with the experiment.[19] The case also occurred on adsorption structures **22**, **25**, **26**, **27**, and **39**, as discussed below.

In **20** and **21**, the Mo−N distances are 1.888 and 1.833 Å, respectively, and the N−O bond lengths are 1.170 and 1.181 Å, respectively. On the basis of the N−O bond lengths, the adsorbed NO in **21** is more activated than that in **20**. In **20**, the Mo(c)−S distance (2.477 Å) is longer than that of $Mo_{16}S_{34}$ (2.288 Å), while the Mo(e)−S(c) and Mo(e)−S(e) distances become shorter and longer (2.345 vs 2.608) than those of $Mo_{16}S_{34}$ (2.448 vs 2.381 Å). In **21**, the terminal Mo(c)−S distances are 2.142 Å.

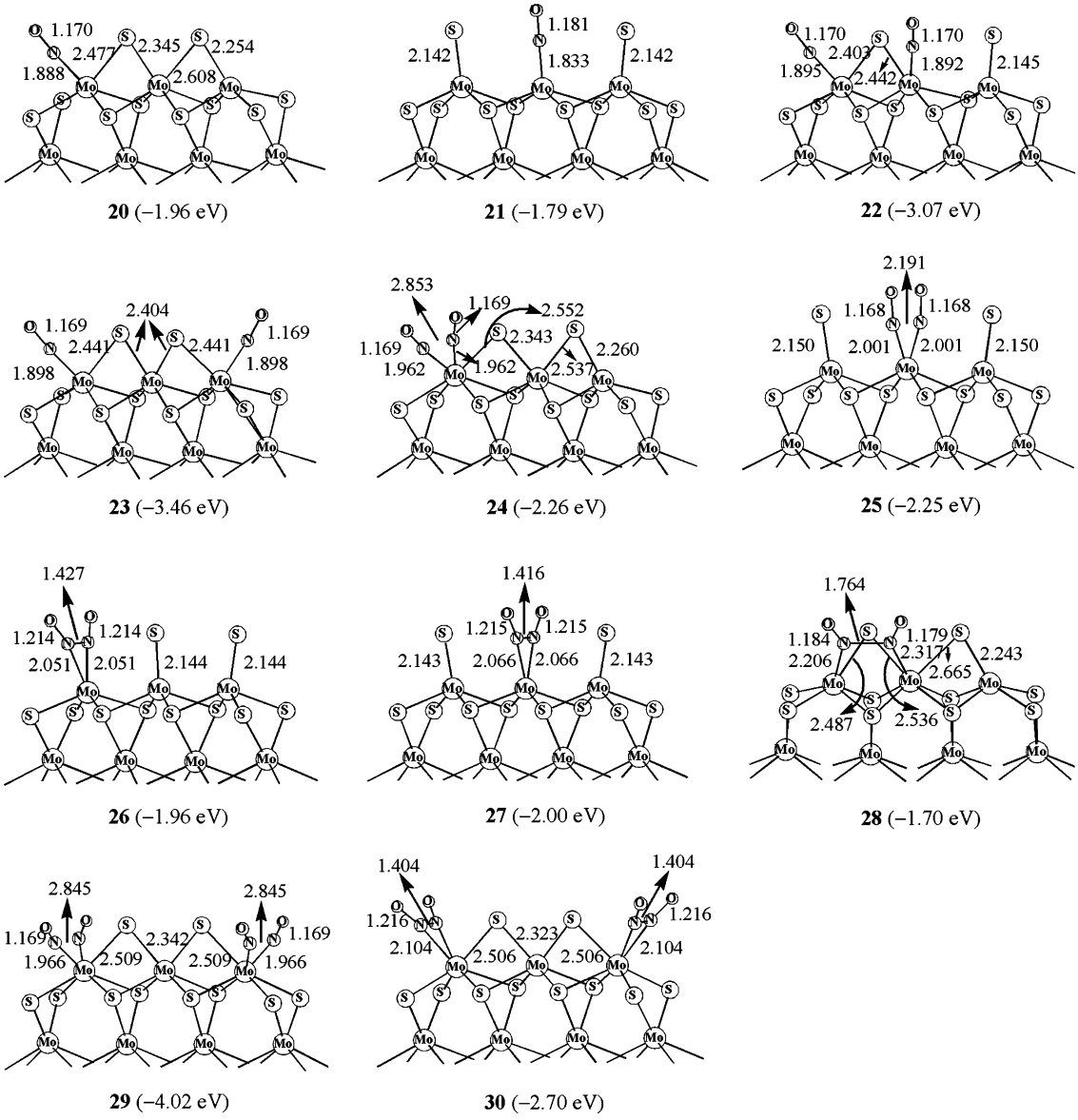

Figure 4. Optimized NO adsorption structures on the $Mo_{16}S_{34}$ cluster.

TABLE 2: Calculated NO Adsorption Energies on the $Mo_{16}S_{34}$ Cluster (E_{ads}, eV) and ΔE_{ads}, eV), as Well as the NO Vibrational Frequency (cm^{-1})

model	E_{ads} (ΔE_{ads})	ν (NO)
	One NO Adsorption	
20	−1.96	1783
21	−1.79	1712
	Two NO Adsorption	
22	−3.07 (+0.68)	1756[a]/1778[b]
23	−3.46 (+0.46)	1784[a]/1788[b]
24	−2.26 (+1.66)	1743[a]/1775[b]
25	−2.25 (+1.33)	1698[a]/1793[b]
26	−1.96 (+1.96)	1554[a]/1532[b]
27	−2.00 (+1.58)	1543[a]/1515[b]
28	−1.70 (+2.05)	1644[a]/1683[b]
	Four NO Adsorption	
29	−4.02(+0.50)	1746[a]/1781[b] (corner)
30	−2.70 (+1.22)	1531[a]/1503[b] (corner)

[a] Asymmetric stretching frequencies. [b] Symmetric stretching frequencies.

Compared with the adsorptions on $Mo_{16}S_{32}$ (Table 1), the adsorption on $Mo_{16}S_{34}$ is by far weaker. The NO frequency (1783 cm^{-1}) of **20** is close to the experiment data of 1775 cm^{-1} by Maugé et al.[12] For the adsorption energy and the calculated frequency, one can see that **20** with one NO adsorption on the corner of the $Mo_{16}S_{34}$ cluster is favorable.

(b) Two NO Adsorption. Adsorption of two NO probes is also studied on the Mo edge of the $Mo_{16}S_{34}$ cluster. As shown in Figure 4, there are seven structures (**22**−**28**) for the adsorption of two NO probes on the $Mo_{16}S_{34}$ cluster. Structures **22** and **23** have two adsorbed NO probes on the corner/edge and corner/corner sites, respectively. In **22**, one of the bridge S on the Mo edge is converted into terminal sulfur, but another bridge S is still adsorbed on two Mo atoms. Structure **23** can be considered as the combination of two **20**, and the adsorption energies of **23** are lower than the two times of **20** (−3.46 and −3.92 eV, respectively), indicating the repulsive interaction of the germinal adsorbed NO probes.

Structures **24** and **25** have dinitrosyl species on the corner and edge Mo atoms, respectively, but their adsorption energies (−2.26 and −2.25 eV, respectively) are much lower than the sum of two **20** and two **21** (−3.92 and −3.58 eV, respectively), indicating the strong repulsive interaction of the germinal adsorbed NO probes. Apart from the terminal adsorption in **24** and **25**, we have computed the adsorption of the $(NO)_2$ dimer.

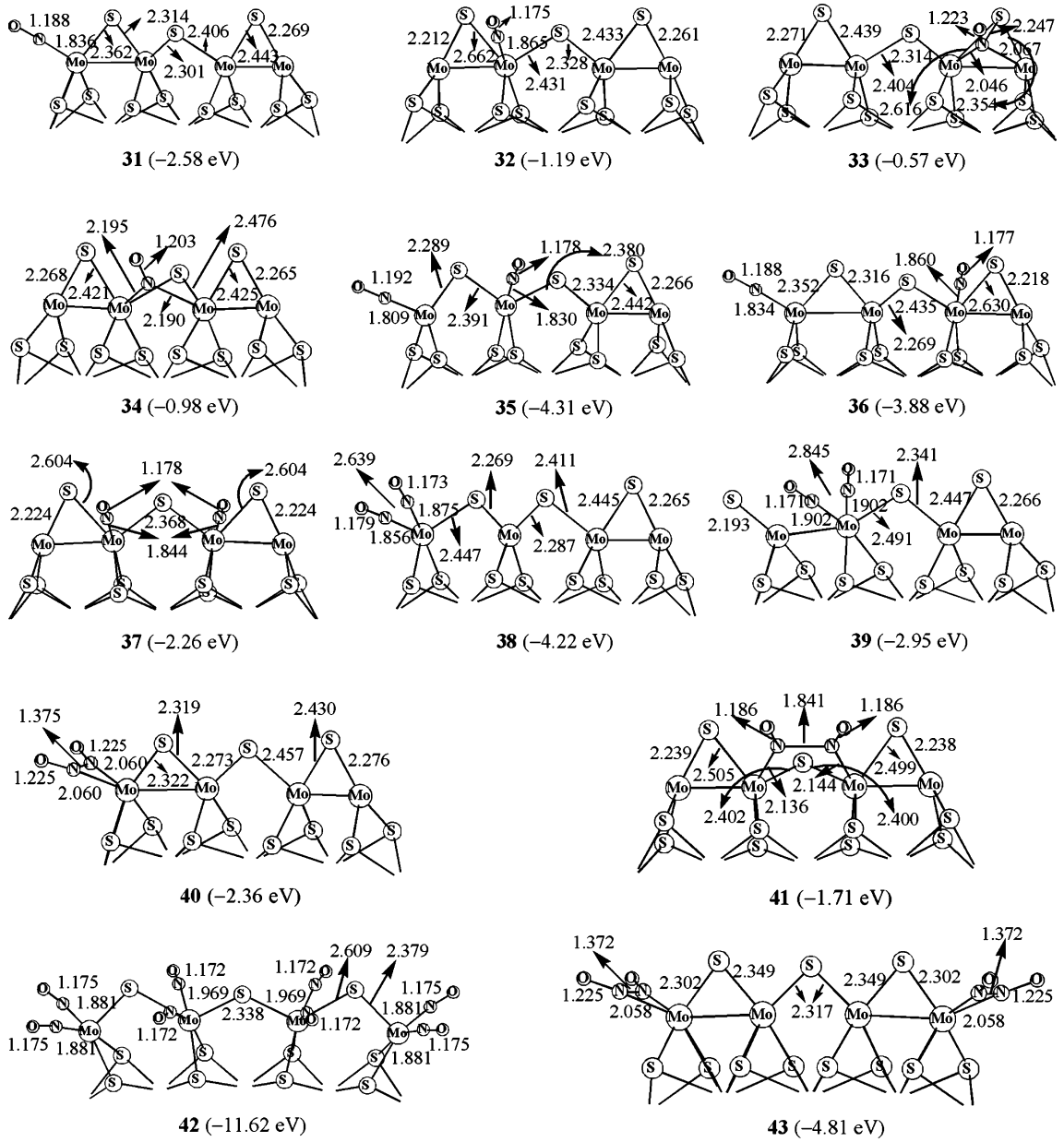

Figure 5. Optimized NO adsorption structures on the $Mo_{16}S_{29}$ cluster.

Structures **26** and **27** show the NO dimer species adsorbed on the corner and on the edge Mo atom, while **28** has adsorbed $(NO)_2$ bridging the corner and edge Mo sites. The N−N distance is 1.427 Å in **26** and 1.416 Å in **27**, but longer in **28** (1.764 Å). The adsorption energies (−1.96 and −2.00 eV) of **26** and **27** are higher than that (−1.70 eV) of **28**. It is interesting to note that NO adsorption in **25**, **26**, and **27** on the 50% sulfur Mo edge changes the bridge S into a terminal sulfur.

As given in Table 2, among the seven adsorption structures of two adsorbed NO probes, all adsorptions are exothermic, indicating the thermodynamic possibility for the second NO adsorption on the $Mo_{16}S_{34}$ cluster, and **23** is the most stable adsorption mode with two adsorbed NO probes on the corner Mo atoms, followed by **22** (−3.07 eV) with two NO probes on one corner and edge Mo atom, while other structures are much less stable. For **23**, the Mo(c)−S and Mo(e)−S distances are 2.441 and 2.404 Å, respectively, and longer and shorter than those of $Mo_{16}S_{34}$ (2.288 vs 2.538 Å), respectively. In **22**, one of the bridge S converts into terminal sulfur with the distance of 2.145 Å. For the bridge S in **22**, the Mo(c)−S and Mo(e)−S distances are 2.403 and 2.442 Å, respectively.

It is interesting to note that the ΔE_{ads} values for all these adsorption structures are positive (Table 2), indicating the repulsive interaction of the adsorbed NO probes. On the basis of these results, it is proposed that dinitrosyl and dimer species are less possible at low NO coverage.

The frequencies for all adsorbed NO probes are calculated (Table 2). In experiment, Maugé et al.[12] ascribed the couple of NO IR bands at 1855 and 1756 cm^{-1} to the weakly bound dinitrosyl species on the surface of MoS_x, and another pair of broader bands at 1775 and 1675 cm^{-1} to the $(NO)_2$ dimer species. In our calculation, the frequencies of **22** (1756/1778 cm^{-1}) and **23** (1784/1788 cm^{-1}) are close to the experimental data (1756 and 1775 cm^{-1}) of Maugé et al.[12] For the dinitrosyl species in **24**, the symmetric frequencies (1775 cm^{-1}) are close to the experimental data (1775 cm^{-1}). However, the frequencies of **25** with dinitrosyl adsorption on the edge Mo (1698 and 1793 cm^{-1}) do not agree with the data (1855 and 1756 cm^{-1}) of Maugé et al.,[12] but are close to the values (1704 and 1795 cm^{-1}) of Valyon et al.[9,10] In addition, the frequencies for the NO dimer in **26** (1554/1532 cm^{-1}) and **27** (1543/1515 cm^{-1}) are lower

TABLE 3: Calculated NO Adsorption Energies on the $Mo_{16}S_{29}$ Cluster (E_{ads}, eV) and ΔE_{ads}, eV), as Well as the NO Vibrational Frequency (cm^{-1})

model	E_{ads} (ΔE_{ads})	ν (NO)
	One NO Adsorption	
31	−2.58	1700
32	−1.19	1750
33	−0.57	1473
34	−0.98	1550
	Two NO Adsorption	
35	−4.31 (−0.54)	1694[a]/1734[b]
36	−3.88 (−0.11)	1695[a]/1739[b]
37	−2.26 (+0.12)	1735[a]/1748[b]
38	−4.22 (+0.94)	1729[a]/1793[b]
39	−2.95 (−0.57)	1740[a]/1776[b]
40	−2.36 (+2.80)	1502[a]/1504[b]
41	−1.71 (+0.67)	1596[a]/1654[b]
	Eight (or Four) NO Adsorption	
42	−11.62 (+2.72)	1734[a]/1788[b] (corner) 1725[a]/1739[b] (edge)
43	−4.81 (−0.09)	1502[a]/1507[b] (corner)

[a] Asymmetric stretching frequencies. [b] Symmetric stretching frequencies.

than the experimental data of Maugé et al.,[12] and the frequencies in **28** (1644/1683 cm^{-1}) are close to the experimental data (1675 cm^{-1}).

(c) NO Adsorption at Higher Coverage. On the basis of the previous calculations, we have considered the full adsorption on both corner and side with totally six NO probes, but two NO probes on the side site escaped, and only four adsorbed NO probes on $Mo_{16}S_{34}$ cluster are possible. Structure **29** with two dinitrosyl species and **30** with two dimer species are in Figure 4. The adsorption energy of **29** is −4.02 eV and the ΔE_{ads} value is positive by +0.50 eV, while the adsorption energy and the ΔE_{ads} value of **29** are −2.70 and +1.22 eV, respectively, and this indicates the thermodynamically unfavorable process for adsorption of two dimer species at high coverage. The calculated asymmetric and symmetric frequencies are 1746 and 1781 cm^{-1} for the corner dinitrosyl in **29**, as well as 1531 and 1503 cm^{-1} for the corner dimer in **30**, respectively. The calculated frequencies in **29** agree with the experiment data (1756 and 1775 cm^{-1}) of Maugé et al.[12] However, the calculated frequencies for dimer species in **30** do not agree with these data from both Maugé et al.[12] and Valyon et al.[9,10]

3.3. NO Adsorption on $Mo_{16}S_{29}$ Cluster. The adsorption structures for one NO, two NO, and six (or four) NO adsorbed on the $Mo_{16}S_{29}$ cluster with 50% sulfur coverage have been discussed, as shown in Figure 5. These adsorption energies are listed in Table 3.

(a) One NO adsorption. As shown in Figure 5, four single NO adsorption structures (**31**−**34**) are obtained. Structures **31** and **32** have corner and edge adsorptions, while **33** and **34** have adsorbed NO bridging two Mo centers. As given in Table 3, all adsorptions are exothermic. Terminal adsorptions **31** and **32** (−2.58/−1.19 eV) are stronger than bridge adsorptions **33** and **34** (−0.57/−0.98 eV). The computed adsorption energies in Table 3 identify **31** (−2.58 eV) with one NO adsorption on the corner as the most favored form. In **31** and **32**, the Mo−N distances are 1.836 and 1.865 Å, and the N−O bond lengths are 1.188 and 1.175 Å, respectively (Figure 5). In **33**, the Mo(c)−N and Mo(e)−N distances are 2.067 and 2.046 Å, respectively. The two Mo(e)−N distance are 2.195 and 2.190 Å in **34**. The N−O bond length is 1.223 Å in **33** and 1.203 Å in **34**, longer than that in **31** and **32**. On the basis of the bond lengths, the adsorbed NO in **33** and **34** is more activated.

Figure 5 shows also the change of the surface structure after adsorption. In comparison with the bare $Mo_{16}S_{29}$ cluster in Figure 1, the Mo(c)−S(c) and Mo(e)−S(c) distances in **31** become longer and shorter after NO adsorption (2.362/2.314 vs 2.260/2.448 Å), while the Mo(e)−S(c) and Mo(e)−S(e) distances in **32** become longer than those of $Mo_{16}S_{29}$ (2.662/2.431 vs 2.448/2.381 Å), respectively.

The computed frequencies of **31** (1700 cm^{-1}) and **32** (1750 cm^{-1}) are in the range of the experimental data of 1704 cm^{-1} by Valyon et al.[9,10] and 1756 cm^{-1} by Maugé et al.,[12] while those of two bridge adsorption (1473 and 1550 cm^{-1}) are much lower.

(b) Two NO Adsorption. Adsorption of two NO probes is also studied on the 50% sulfur S edge. As shown in Figure 5, there are seven double NO adsorption structures (**35**−**41**) on $Mo_{16}S_{29}$, and the adsorption energies are listed in Table 3. All adsorption are exothermic, indicating the possibility for the 50% sulfur S edge to adsorb one additional NO molecule. Structures **35** and **36** have two adsorbed NO probes on the corner/edge sites, and **37** with two adsorbed NO probes on two edge Mo atoms. Structures **35** and **36** can be considered as the combination of **31** and **32**, and their adsorption energies are lower than the sum of **31** and **32** (−4.31 and −3.88 vs −4.77 eV), indicating the repulsive interaction of the adsorbed NO probes. As shown in Figure 5, **38** and **39** have dinitrosyl adsorption on corner and edge Mo sites, respectively, but their adsorption energies (−4.22 and −2.95 eV) are higher than the sum of two **31** (−4.16 eV) and **32** (−2.38 eV), indicating the affinity for two NO adsorption. Apart from the dinitrosyl species adsorption in **38** and **39**, it is notable that there is also adsorption of the $(NO)_2$ dimer. Structure **40** show the NO dimer species adsorbed on the corner, while **41** has adsorbed $(NO)_2$ bridging corner and edge Mo sites. However, the structure with NO dimer species adsorption on edge Mo atom is not obtained, and optimization led to **39** with dinitrosyl species on the edge Mo atom. The N−N and N−O distances are 1.375 and 1.225 Å in **40**, and 1.841 and 1.186 Å in **41**, respectively. From Table 3, the ΔE_{ads} value is positive for **40** and **41**, indicating a repulsive effect.

On the basis of these adsorption energies, **35** (−4.31 eV) is the most stable mode with one corner NO and one edge NO, followed by **38** (−4.22 eV) with dinitrosyl species on the corner Mo atom, and **36** (−3.88 eV) with NO on one corner and one next edge Mo. The adsorption in **40** for NO dimer species in the corner Mo edge is weaker than that for dinitrosyl species on same site (**38**), and the adsorption of the second dimer species (**41**) is also weaker than the corresponding two NO in **37**.

The calculated frequencies of the adsorbed NO probes are given in Table 3. The frequencies of **31** and **32** are 1700 and 1750 cm^{-1}, respectively. The frequencies for NO on the corner Mo and on the edge Mo are 1694 and 1734 cm^{-1} in **35**. The frequencies for **37** (1735/1748 cm^{-1}), **38** (1729/1793 cm^{-1}), and **39** (1740/1776 cm^{-1}) are in the characteristic ranges of 1756 and 1775 cm^{-1} by Maugé et al.[12] and 1794 cm^{-1} by Valyon et al.[9,10]

(c) Adsorption at Higher Coverage. On the basis of the most favored adsorption modes discussed above, we have considered the full NO adsorption on $Mo_{16}S_{29}$ cluster by totally eight NO probes, as shown in structure **42** in Figure 5. In addition, we have also tried to get the corresponding structure with four dimer NO species, but optimization led only to structure **43** with two NO dimer species at the corner and the four NO probes at the edge site escaped. The adsorption energy of **42** is −11.62 eV, and the ΔE_{ads} value is positive by +2.72 eV, indicating the

repulsive interaction (Table 3). In addition, the adsorption energy and the ΔE_{ads} value of **43** are −4.81 and −0.09 eV, respectively. The rather lower NO adsorption energy of **43** reveals that the dimer form should be not formed at high coverage. The dinitrosyl and dimer NO frequencies differ strongly. In **42**, the asymmetric and symmetric frequencies for the corner dinitrosyl are 1734 and 1788 cm^{-1}, and for the edge dinitrosyl species are 1725 and 1739 cm^{-1}, respectively. In **43**, the asymmetric and symmetric frequencies of the corner NO dimer are 1502 and 1507 cm^{-1}, respectively, and lower than those of dinitrosyl species.

4. Conclusion

NO probe adsorptions on the stoichiometric $Mo_{16}S_{32}$ and nonstoichiometric $Mo_{16}S_{34}$ and $Mo_{16}S_{29}$ clusters have been investigated by using the density functional theory method. Although the formation of the naked Mo edge is not favored energetically, the indirect formation of the covered Mo edge with probe molecules (CO or H_2S) can be possible. In addition, the naked Mo edge also provides the opportunity for comprehensive and systematic comparison and understanding of the surface structure and activity of MoS_x catalysts.

On the basis of the calculated adsorption energies, NO adsorption on the Mo edge of the stoichiometric $Mo_{16}S_{32}$ cluster are stronger than those of the nonstoichiometric $Mo_{16}S_{34}$ cluster and those on the S edge of the nonstoichiometric $Mo_{16}S_{29}$ cluster.

For each MoS_x cluster, the adsorption structures of two NO adsorption on different Mo edge are more favorable than those of the corresponding dinitrosyl species and dimer species. There is strong repulsive interaction in dinitosyl and dimer species on the basis of the calculated ΔE_{ads} values. It also is found that monitrosyl adsorptions are more favorable at low NO coverage, while dinitrosyl and dimer adsorptions are possible at higher NO coverage.

Apart from the structures and energies, the NO stretching frequencies have also been computed. For one NO adsorption, the frequencies of NO in $Mo_{16}S_{32}$ cluster **1** (1684 cm^{-1}), **2** (1688 cm^{-1}), and **5** (1659 cm^{-1}) are close to the experimental data (1675 cm^{-1}). The frequencies of NO in $Mo_{16}S_{34}$ cluster (**20**) (1783 cm^{-1}) and $Mo_{16}S_{29}$ cluster (**32**) (1749 cm^{-1}) agree with the characteristic data (1775 and 1756 cm^{-1}). In addition, the frequencies for **21** (1712 cm^{-1}) and **31** (1700 cm^{-1}) are close to experimental value (1704 cm^{-1}).

For two NO adsorption on the MoS_x cluster, the frequencies for **11** and **12** (on $Mo_{16}S_{32}$), **22**, **23**, **24**, and **25** (on $Mo_{16}S_{34}$) and **37**, **38**, and **39** (on $Mo_{16}S_{29}$) are in the range of experiment data. Under full adsorption, the highest frequency of NO adsorption on the MoS_{32} cluster at 1815 cm^{-1} in **16** is closer to the experimental value of (1820 cm^{-1}) found on other surfaces than to the experimental data (1855 cm^{-1}) of Maugé et al. In contrast to the nice agreement between the calculated and detected NO stretching frequencies for mononitrosyl and dinitrosyl adsorptions, the calculated frequencies of the adsorbed $(NO)_2$ dimer species are much lower than the suggested experimental data.

Acknowledgment. This work has been supported by the National Nature Science Foundation of China (20590360 and 20573127).

Supporting Information Available: Total electronic energies for all adsorbed MoS_x clusters are given. This material is available free of charge via the Internet at http://pubs.acs.org.

References and Notes

(1) Kushmerick, J. G.; Kandel, S. A.; Han, P.; Johnson, J. A.; Weiss, P. S. *J. Phys. Chem. B* **2000**, *104*, 2980.
(2) Payen, E.; Hubaut, R.; Kasztelan, S.; Poulet, O.; Grimblot, J. *J. Catal.* **1994**, *147*, 123.
(3) Weber, T.; Muijsers, J. C.; Niemantsverdriet, J. W. *J. Phys. Chem.* **1995**, *99*, 9194.
(4) Plazenet, G.; Cristol, S.; Paul, J.-F.; Payen, E.; Lyncb, J. *Phys. Chem. Chem. Phys.* **2001**, *3*, 246.
(5) Lauritsen, J. V.; Nyverg, M. Nørskov, J. K.; Clausen, B. S.; Topsøe, H.; Lægsgaard, E.; Besenbacher, F. *J. Catal.* **2004**, *224*, 94.
(6) Topsøe, N.-Y.; Topsøe, H. *J. Catal*. **1983**, *84*, 386.
(7) Perl, J. B. *J. Phys. Chem.* **1982**, *86*, 1615.
(8) Okamoto, Y.; Katoh, Y.; Mori, Y. Imanaka, T.; Teranishi, S. *J. Catal.* **1981**, *70*, 445.
(9) Valyon, J.; Hall, W. K. *J. Catal.* **1983**, *84*, 216.
(10) Valyon, J.; Schneider, R.; Hall, W. K. *J. Catal.* **1984**, *85*, 277.
(11) Shuxian, Z.; Hall, W. K.; Ertl, G.; Knözinger, H. *J. Catal.* **1986**, *100*, 167.
(12) Maugé, F.; Lamotte, J.; Nesterenko, N. S.; Manoilova, O.; Tsyganenko, A. A. *Catal. Today* **2001**, *70*, 271.
(13) Topsøe, N.-Y.; Topsøe, H. *J. Catal*. **1982**, *77*, 293.
(14) Yamada, M.; Koizumi, N.; Yamazaki, M. *Catal. Today* **1999**, *50*, 3.
(15) Nielsen, L. P.; Ibsen, L.; Christensen, S. V.; Clausen, B. S. *J. Mol. Catal. A* **2000**, *162*, 375.
(16) Okamoto, Y.; Kawano, M.; Kawabata, T.; Kubota, T. Hiromitsu, I. *J. Phys. Chem. B* **2005**, *109*, 288.
(17) Okamoto, Y.; Kubota, T. *Catal. Today* **2003**, *86*, 31.
(18) Schönnenbeck, M.; Cappus, D.; Klinkmann, J.; Freund, H. J.; Petterson, L. G. M.; Bagus, P. S. *Surf. Sci.* **1996**, *347*, 337.
(19) Nart, F. C.; Friend, C. M. *J. Phys. Chem. B* **2001**, *105*, 2773.
(20) Queeney, K. T.; Friend, C. M. *J. Phys. Chem. B* **1998**, *102*, 9251.
(21) Zecchina, A.; Garrone, E.; Morterra, C.; Coluccia, S. *J. Phys. Chem.* **1975**, *79*, 978.
(22) Liu, Z. P.; Jenkins, S. J.; King, D. A. *J. Am. Chem. Soc.* **2004**, *126*, 7336.
(23) Zeng, T.; Wen, X.-D.; Wu, G.-S.; Li, Y.-W.; Jiao, H. *J. Phys. Chem. B* **2005**, *109*, 2846.
(24) Zeng, T.; Wen, X.-D.; Li, Y.-W.; Jiao, H. *J. Phys. Chem. B* **2005**, *109*, 13704.
(25) Lauritsen, J. V.; Bollinger, M. V.; Lægsgaard, E.; Jacobsen, K. W.; Nøskov, J. K.; Clausen, B. S.; Topsøe, H.; Besenbacher, F. *J. Catal.* **2004**, *221*, 510.
(26) Byskov, L. S.; Nørskov, J. K.; Clausen, B. S.; Topsøe, H. *J. Catal.* **1999**, *187*, 109.
(27) Raybaud, P.; Hafner, J.; Kresse, G.; Toulhoat, H. *Surf. Sci.* **1998**, *407*, 237.
(28) Raybaud, P.; Hafner, J.; Kresse, G.; Toulhoat, H. *Phys. Rev. Lett.* **1998**, *80*, 1481.
(29) Cristol, S.; Paul, J. F.; Payen, E.; Bougeard, D.; Clémendot, S.; Hutschka, F. *J. Phys. Chem. B.* **2000**, *104*, 11220.
(30) Travert, A.; Nakamura, H.; van Santen, R. A.; Cristol, S.; Paul, J. F.; Payen, E. *J. Am. Chem. Soc.* **2002**, *124*, 7084.
(31) Sun, M.; Nelson, A. E.; Adjaye, J. *J. Catal.* **2004**, *226*, 32.
(32) Sun, M.; Adjaye, J.; Nelson, A. E. *Appl. Catal. A* **2004**, *263*, 131.
(33) Wen, X.-D.; Zeng, T.; Li, Y.-W.; Wang, J.; Jiao, H. *J. Phys. Chem. B* **2005**, *109*, 18491.
(34) Paul, J.-F.; Payen, E. *J. Phys. Chem. B* **2003**, *107*, 4057.
(35) (a) Zeng, T.; Wen, X.-D.; Li, Y.-W.; Jiao, H. *J. Mol. Catal. A* **2005**, *241*, 219. (b) Wen, X.-D.; Zeng, T.; Jiao, H. *J. Phys. Chem. B* **2006**, *110*, 14004.
(36) Travert, A.; Dujardin, C.; Maugé, F.; Veilly, E.; Cristol, S.; Paul, J.-F.; Payen, E.; Bougeard, D. *Catal. Today* **2001**, *70*, 255.
(37) (a) Delley, B. *J. Chem. Phys.* **1990**, *92*, 508. (b) Delley, B. *J. Phys. Chem.* **1996**, *100*, 6107. (c) Delley, B. *J. Chem. Phys.* **2000**, *113*, 7756.
(38) Perdew, J. P.; Wang, Y. *Phys. Rev. B* **1992**, *45*, 13244.